Advances in ungauged streamflow prediction using artificial neural networks

Lance E. Besaw[1§], Donna M. Rizzo[1], Paul R. Bierman[2] and William Hackett[2]

[§]Corresponding Author

[1]School of Engineering and Mathematical Sciences, University of Vermont, Votey Hall, 33 Colchester Ave, Burlington, VT

[2]Department of Geology, University of Vermont, Delehanty Hall, 180 Colchester Ave, Burlington, VT

In preparation for submission to the *Journal of Hydrology*

Abstract

Sustainable water resources management is an important issue in developing and established communities; particularly with the challenges associated with surface and groundwater contamination and potential precipitation shifts resulting from climate change. In this work, we develop and test methods to forecast streamflow in ungauged basins using counterpropagation and generalized regression artificial neural networks (ANNs). These were selected due to their advantages over other data-driven ANNs; namely their training speed and guaranteed convergence. The ANN models are driven with inputs of local climate records and antecedent streamflow predictions (through a recurrent feedback loop). The incorporation of this feedback loop allows the ANNs to forecast flow in ungauged basins, where no flow observations are available. These methods are compared with traditional, data-driven flow forecasting models (multiple linear regression and autoregressive moving average with exogenous inputs), where applicable. Climate and USGS streamflow records from three basins in Northern Vermont are used to test and compare the methods. To validate the prediction of flow in ungauged basins, the ANNs are trained on climate-flow data from one basin and to forecast streamflow in a nearby basin, with a different climate record. Results reveal that training and predicting with data from nearby basins produce accuracies that are not statistically different than those attained when training and predicting in the same basin. In addition, a comparison of the ANN prediction accuracies using data collected on two time scales (daily and hourly) is presented.

Keywords: ungauged streamflow forecasts, artificial neural networks, time series analysis, counterpropagation, generalized regression neural network.

1. Introduction

Accurate streamflow forecasts are an important component of watershed planning and sustainable water resource management. Streams and rivers adjust during large flood events, sometimes with catastrophic damage to human infrastructure; and riverine ecosystems are often most susceptible during periods of low flow. The magnitude and locality of extreme events can result in degraded surface water quality, loss of agricultural lands, damaged infrastructure, and the mobilization of phosphorus and sediment-related pollutants. The frequency and severity of these extreme events are exacerbated by climate change and anthropogenic factors. Accurate and timely predictions of high and low flow events at any watershed location (either gauged or ungauged) can provide stakeholders the information required to make strategic, informed decisions.

Data-driven hydrological methods have been widely adopted for forecasting streamflow. Such techniques often require similar data types as traditional physics-based models, but require much less development time and are useful for real-time applications. Despite their lack of physical interpretation to basin-scale physics, they have proven capable of accurately predicting flows. Multiple linear regression (MLR) and variations of autoregressive moving average (ARMA) models are common data-driven methods for forecasting streamflow. More recently, artificial neural networks (ANNs) have been adopted to forecast flow.

In this paper, we add to previous ANN research for forecasting streamflow using climactic and hydrologic drivers. However, we focus on a methodology that can be applied to forecast flow in ungauged basins because it does not use measured streamflow as an input variable. Instead, input variables include precipitation and temperature data in combination with flow predictions lagged in time. To validate the method, we compare the two proposed ANN algorithms (recurrent generalized regression neural network (GRNN) and counterpropagation (CPN)) with traditional data-driven methods (MLR and ARMA), where applicable. The CPN and GRNN algorithms have been selected because they are fast, easy to train, always converge and are widely applicable to smaller watersheds.

2. Background

The functional relationship between rainfall and streamflow is complex and highly non-linear. It is influenced by the temporal and spatial distribution of rainfall, watershed topography, soil characteristics, and mechanisms by which surface water recharges groundwater, among other factors. It has long been an objective of researchers and watershed managers alike to accurately forecast this complex and highly non-linear process.

Water resource practitioners have primary used simple linear regression or time series models to forecast time-series hydrological processes (Maier and Dandy, 2000). There are numerous hydrological applications in which regression methods are used (e.g. Tangborn and Rasmussen (1976), Phien et al. (1990) and Tolland et al. (1998), among others). More recently, Schilling and Wolter (2005) use multiple linear regression to predict streamflow using a wide range of input variables, including short-term temporal inputs like precipitation and basin scale characteristics like land use, geology and morphology. Hsieh et al. (2003) find similar predictive capabilities between multiple linear regression and feedforward neural networks when relating Columbia River streamflow with large-scale climatologic variables (e.g. Pacific sea surface temperatures).

Time series autoregressive moving average or ARMA models (Box and Jenkins, 1970) are also used for hydrological estimation applications (e.g. Chaloulakou (1999), McKerchar and Delleur (1974), and Yurekli et al. (2005), among others). New forecasting methods have been compared with the ARMA-family of models (Firat (2008), Adamowski (2008), and Cigizoglu (2003)), and autoregressive moving average with exogenous input (ARMAX) models; the latter being used to incorporate precipitation data to forecast streamflow. Chang and Chen (2001) use an ARMAX model to evaluate the predictive capabilities of their fuzzy-counterpropagation ANN, while Hsu et al. (1995) found that ANN predictions of stream flow outperform linear ARMAX.

Over the past two decades, there has been a growing interest in ANNs for simulating and forecasting hydrological variables (Govindaraju, 2000a; Govindaraju, 2000b). Govindaraju and Ramachandra (2000) provide a broad introduction to the application of ANNs in hydrology up to 2000. Several ANN algorithms have been used, including feedforward backpropagation (FFBP), radial basis function (RBF) (Kisi, 2008; Moradkhani et al., 2004; Singh and Deo, 2007), and self-organizing maps (SOMs) (Hsu et al., 1995; Hsu et al., 2002).

Studies have explored a multitude of input variables to increase flow forecasting accuracies. Makkersorn et al. (2008) include sea surface temperatures and spatio-temporally distributed rainfall data to forecast streamflow, using genetic programming and FFBP ANN methods. Singh and Deo (2007) compare several ANN algorithms and generate separate ANN models for each season. Kisi (2008) includes a periodicity component (month enumerator) as an input to their ANN models to predict monthly streamflow. Rajurkar et al. (2002) improved their predictive results by forecasting at the sub-catchment rather than the entire catchment scale (due to spatial variation of rainfall). Cigizoglu and Kisi (2005) used a GRNN model to estimate upstream daily intermittent river flows using downstream data.

Other ANN advancements have proven useful in predicting flow. Several authors use an adaptive neuro-fuzzy inference system (ANFIS), which combines fuzzy logic principles (Zadeh, 1965) and ANNs, to forecast streamflow (Chang and Chen, 2001; Chang et al., 2001; Firat, 2008; Firat and Gungor, 2008). Other studies found success using recurrent FFBP algorithms (Chang et al., 2002; Connor et al., 1994).

Despite the abundance of streamflow forecast ANN literature, more than 95% of the researchers (32 of 33 papers referenced here) use antecedent *observations* of streamflow and precipitation (or other climatic variables) to forecast streamflow (e.g. (Firat and Gungor, 2008; Hu et al., 2005; Imrie et al., 2000; Jeong and Kim, 2005; Kisi, 2005)). One notable exception is Wang et al. (2006), who use several modified FFBP ANNs to predict streamflow with a 1 to 10 day lead-time. To do so, they implement a recursive algorithm in which future streamflow predictions, say $\hat{Q}(t+2)$, are based on predicted streamflow, say $\hat{Q}(t+1)$.

The feed-forward backpropagation (FFBP) algorithm is by far the most commonly used method in streamflow estimation (e.g. (Khalil et al., 2005; Rajurkar et al., 2002; Zealand et al., 1999)). Kingston et al. (2005) and Maier and Dandy (2000) provide good reviews. However, this algorithm requires stochastic training, does not always converge, and is widely considered a black-box approach to hydrological modeling (Kingston et al., 2005). To circumvent these challenges, this study focuses on two ANN algorithms that are not stochastic in nature and do not require iterative training procedures: the counterpropagation network (CPN) and the generalized regression neural network (GRNN). The CPN has been used with concepts of fuzzy logic to predict hourly streamflow (Chang and Chen, 2001) and to develop fuzzy classification rules that accurately reconstruct streamflow (Chang et al., 2001). The GRNN has been shown to outperform FFBP ANN and ARMA methods to predict daily (Cigizoglu, 2005a) and monthly streamflow (Cigizoglu, 2005b), respectively. Kisi (2008) also found the GRNN to be a superior estimator of monthly streamflow than FFBP and RBF ANNs. Aytek (2008) use GRNNs as a basis for comparing a novel evolutionary computation algorithm for prediction streamflow. In addition, only a few researchers have looked to train ANNs on one basin and make predictions in another (e.g. (Cigizoglu, 2003; Kisi, 2008)). However, all of the studies use antecedent flow observations as inputs.

2.1. Study site

The Winooski basin has a warm summer continental or Hemiboreal climate (Koppen classification Dfb), with warm, humid summers and cold winters. The average annual precipitation in the basin is about 100 cm (Hijmans et al., 2005). Land cover within the basin is largely forested in the upper regions, while moderate development is primarily located in the stream valleys (Albers, 2000; Hackett and Bierman, 2009a). Bedrock is primarily schist and phyllite in the mountains with Cambro-Ordivician siliclastic rocks and carbonates to the west in the Champlain Valley Region (Doolan, 1996). There is an abundance of glacial till at elevation, stratified glacial sediments in the valleys, and alluvium near river channels. Unconsolidated cover varies widely throughout the basin, with less material at the higher elevations and more in the valleys.

The Winooski River basin, located in northwestern Vermont, USA, was selected to demonstrate the implementation of these forecasting algorithms. The cumulative area of the Winooski basin is 3,000 km^2 with a main branch length of 142 km. The river originates in the Green Mountains and receives flow from five major tributaries before discharging into Lake Champlain (Figure 1). The Mad River, Dog River, Little River, and North Branch and main stem of the Winooski River are all monitored by USGS stream gauging stations, while the Huntington River remains ungauged.

This study uses hourly and daily streamflow data from three USGS gauging stations and climate data from three NCDC weather stations located within the basin (Figure 1). Although trends (including the NAO cycle) have been observed within the Winooski River basin climate-discharge record (Hackett and Bierman, 2009b), the prediction focus of this study is on a small enough timescale to warrant such trends negligible.

2.1.1. Climate and streamflow data

Although more than 70 years of flow and climate data exists for this basin, daily streamflow at the three USGS sites and climate data at three NCDC weather stations has been gathered from 1996-2006. Streamflow, Q, in m^3/s is an average over the entire day of instantaneous observations. Climate data consists of daily average temperature, T, in ^oC and total precipitation, P, in cm/day. Since not all sub-basins contain a NCDC weather station, precipitation records associated with the nearest NCDC station are assigned to the USGS stations. Thus the Dog River USGS gauging station uses the Northfield NCDC precipitation record and the Winooski River at Wrightsville and Montpelier use the Barre/Montpelier Airport NCDC precipitation record. Temperature data from the Burlington International Airport was adjusted for elevation and approximated at the USGS stations (Citation).

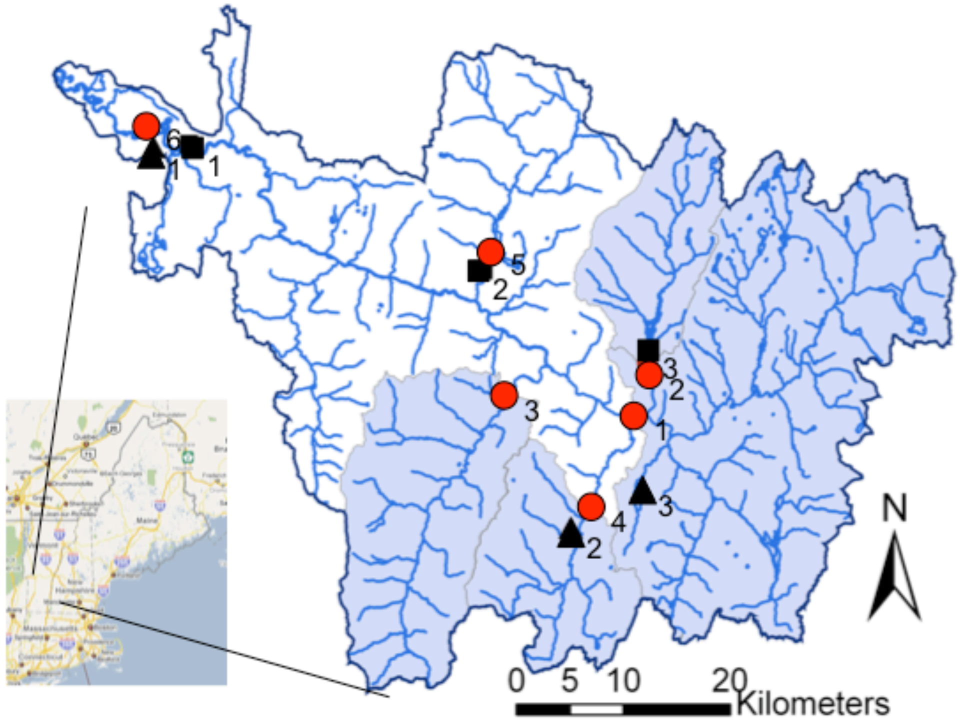

	Station ID	Description	Elev. (m)	Area (km²)
● 1	USGS 04286000	Winooski River at Montpelier	152	1028
● 2	USGS 04285500	Winooski River at Wrightsville	168	179
● 3	USGS 04288000	Mad River at Moretown	166	360
● 4	USGS 04287000	Dog River at Northfield Falls	184	197
● 5	USGS 04290500	Winooski River at Essex Jct.	56	2704
● 6	USGS 04289000	Little River near Waterbury	130	287
▲ 1	NCDC 431081	Burlington International Airport	101	--
▲ 2	NCDC 435733	Northfield	204	--
▲ 3	NCDC 435278	Barre/Montpelier Airport	343	--
■ 1	NID VT0045	Essex Jct. Dam	80	2,693
■ 2	NID VT0027	Little River Reservoir	180	282
■ 3	NID VT0052	Wrightsville Reservoir	196	176

Figure 1. The Winooski River basin and associated USGS gauging and NCDC weather stations (NEED to redo NE portion in GIS). (NID – National Inventory of Dams)

In addition to the daily data, hourly precipitation (cm/hr) and streamflow (m^3/s per hour) data were gathered for the Dog River basin from 1996-2006. Figure 2 shows the Dog River hydrograph and hyetograph for the summer months of 2002. The data is displayed at two scales, hourly (Figure 2a) and daily (Figure 2d). A single storm event occurring on September 28th, 2002 is highlighted at both scales (Figure 2b and e respectively).

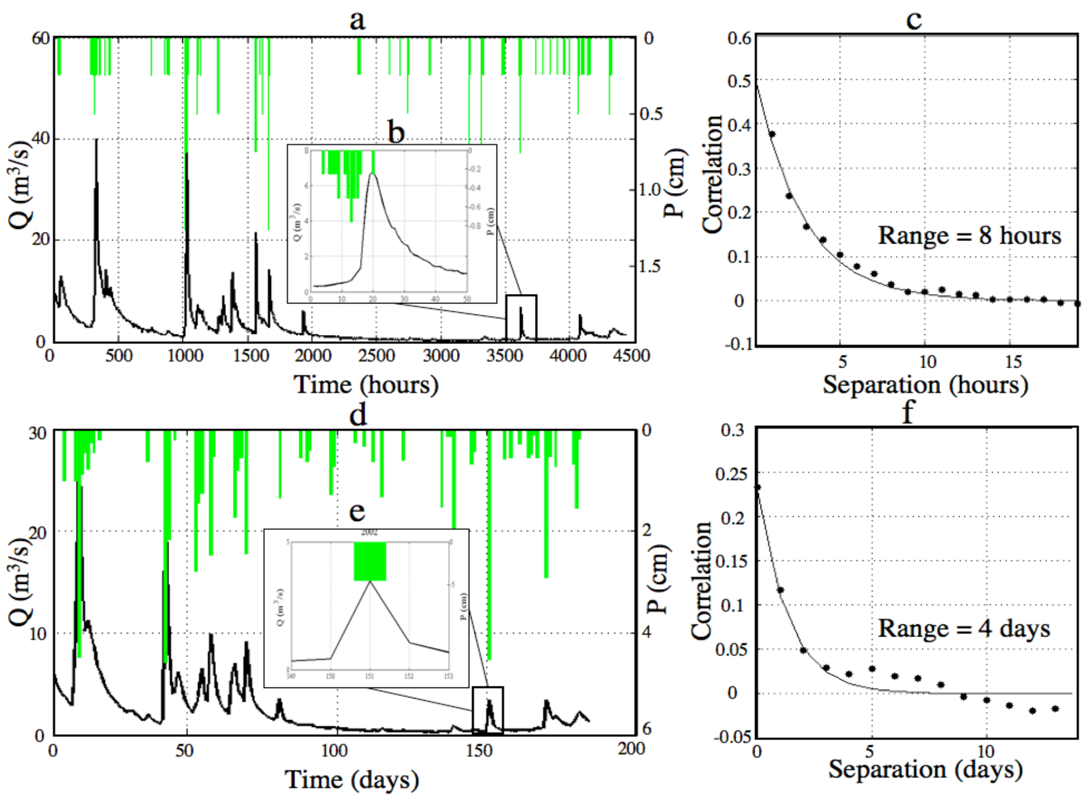

Figure 2. Summer data 2002. (a) Hydrograph and hyetograph for the hourly and (d) daily flow, *Q*, and precipitation, *P*, records. Inset showing (b) hourly and (e) daily Q and P for an individual storm event occurring September 28th. The *P-Q* cross-correlograms (c) and (f) have been used to determine the temporal relationship (time lag) between *P* and *Q*.

In a few studies involving flow forecasting, time series correlation analysis has been used to determine the temporal lag (number of time steps) necessary for the input variables. Moradkhani et al. (2004) looked at the auto-correlation of streamflow and cross-correlation of precipitation-streamflow and temperature-streamflow over two seasons, winter-spring and summer-fall to explore the time dependence among the hydrologic variables. Cigizoglu (2005b) and Kisi (2005) used flow auto-correlations to select the optimal time lag (time steps) of input variables.

In this study, cross-correlation analyses determined the temporal relationship between the precipitation and streamflow (hourly and daily data in Figure 2c and Figure 2f, respectively). Observed decorrelation ranges were estimated to be 8 hours and 4 days respectively. Additional time-series correlation and hydrograph analyses (not shown) were used to determine the optimal number of input variables, Table 1. The same time-lagged variables are used as inputs to all flow forecasting models.

Table 1. Lag times for hourly and daily models.

Variable	Hourly (hrs)	Daily (days)
P	8	4
T	24*	1
Q	4	2

*Temperature is not available at the hourly timescale.

3. Methods

As this work focuses on data driven methods for predicting flow, input-output data pairs are required from which to extract and utilize non-linear, climate-flow relationships. These data pairs consist of antecedent precipitation, climate and flow inputs and flow outputs. The data is separated into training and prediction sets. Data pairs from 1996-2003 are used for training/model development while data from 2004-2006 are used to make predictions and evaluate the different forecasting methods.

In regions with distinct seasonal effects, separate seasonal ANNs have been found to produce the best results (Kisi, 2008; Singh and Deo, 2007). For example one ANN could be trained to accommodate snow and snowmelt and another for high (or low) flow events over summer months. This work focuses only on forecasting summer streamflow resulting from rainstorm events (where "summer" is defined as the months from May to

October). To reduce training and prediction errors (e.g. predicting flows with no precipitation record), dates with missing rainfall and/or precipitation events have been removed from the record (typically days to weeks).

3.1. Generalized regression neural network (GRNN)

Traditionally, the multiple linear regression (MLR) models are the most popular method for predicting streamflow of the form $\hat{Q} = a_1 x_1 + a_2 x_2 + ... + a_n x_n + \varepsilon$, where x_1, $x_2,\ldots x_n$ are the independent input variables (e.g. P, T and Q), a_1, $a_2,\ldots a_n$ are the regression coefficients best fit using a minimum least squares error, ε, between predicted $\hat{Q}$ and observed Q.

Developed as a non-parametric extension of MLR, the GRNN is a memory-based network capable of estimating continuous variables (Specht, 1991). It has a single-pass training algorithm and can be conceptualized as a nonlinear, non-parametric regression, algorithm (Figure 3). The hourly streamflow prediction model is used here to describe the GRNN.

The GRNN consists of four nodal layers: input, pattern, summation and output. It is used to regress streamflow, Q, based on a set of input variables, $\mathbf{x}$, defined by some non-linear function $Q = f(\mathbf{x})$, captured by the training data. Training data consists of set of input vectors, $\mathbf{x}$, and corresponding observed flow, Q. Input vectors consist of 13 predictor variables, $\mathbf{x}(t)$=[$P(t$-1),…$P(t$-8), $T(t$-1), $\hat{Q}(t-1),\ldots \hat{Q}(t-4)$] while the output is a prediction of streamflow. Observed and predicted streamflows are denoted $Q(t)$ and $\hat{Q}(t)$ respectively. The time variable t has been suppressed to simplify the following notation.

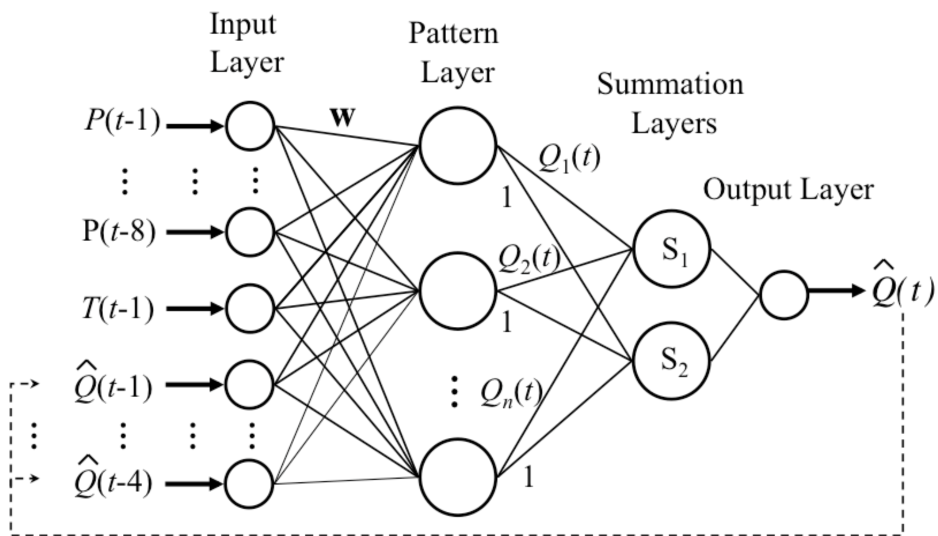

Figure 3. Architecture of the hourly streamflow generalized regression neural network (GRNN) with optional recurrent (feedback) connection (dashed arrow).

Each layer is fully connected to the adjacent layers by a set of weights (or arcs) between nodes. The pattern layer has one node for each n training pattern (input-output pairs). The weights on the left side of the pattern nodes store (e.g. are set equal to) the input training vectors, $\mathbf{x}$, while the weights on the right side store the associated streamflows, Q, for all n training patterns (hence no iterative training is necessary). Each node in the pattern layer is connected to the two summation layer nodes, S_1 and S_2. The weights linking the pattern layer nodes with summation node S_1 store the streamflows (Q_1, Q_2, …Q_n) for each input-output training patterns. The weights from the pattern layer nodes to summation node S_2 are set equal to 1.

With the weights set, the GRNN may be used to make a prediction, $\hat{Q}$. An input vector, $\mathbf{x}$, is passed to the pattern layer and the Euclidean distance is computed between the input vector and all pattern weight vectors, $\mathbf{w}$, as: $D_i^2 = (\mathbf{w} - \mathbf{x}_i)^{\mathrm{T}}(\mathbf{w} - \mathbf{x}_i)$, where $\mathbf{w}$ is the weight matrix representing the stored input training data and $\mathbf{x}_i$ is the i^{th} input vector.

The distance between the input vector and stored data, D_i^2, is passed to the summation layers and the prediction is computed as:

$$\hat{Q} = \frac{S_1}{S_2} = \frac{\sum_{i=1}^{n} Q_i \exp\left(-\frac{D_i^2}{2\sigma^2}\right)}{\sum_{i=1}^{n} \exp\left(-\frac{D_i^2}{2\sigma^2}\right)},$$

where σ^2 is a smoothing parameter that is pivotal when estimating $\hat{Q}$. A large value for σ^2 smoothes the regression surface and produces estimates that approach the sample mean; while a smaller value produces a surface with greater chance of discontinuity resulting in nearest neighbor estimates. Intermediate values of σ^2 produce well behaved estimates that approximate the joint probability density function of $\mathbf{x}$ and Q (Specht, 1991). The prediction $\hat{Q}$ is a weighted average of all stored response observations (Q_1, Q_2, …Q_n), where each response is weighted exponentially according to its Euclidean distance from input vector $\mathbf{x}_i$. The GRNN algorithm described in this work was written in MatLab V. 7.4.0.287 (R2007a).

We modified the traditional GRNN architecture to allow for the recurrent (feedback) connection (dashed line of Figure 3). With this connection, recently predicted streamflows $\hat{Q}(t\text{-}1)$, $\hat{Q}(t\text{-}2)$,… are passed back to the network input layer and used as an input to predict $\hat{Q}$ (t) at the next time step(s). The modification involves incorporating the observed antecedent streamflow $Q(t\text{-}1)$,… into the training input vector, $\mathbf{x}$=[x_1, x_2, …x_m, $Q(t\text{-}1)$,…] and does not change the GRNN algorithm. It adds information to the input layer when training and making predictions. Therefore, when using the network for prediction, an initial value of $Q(t\text{-}1)$ must be ideally know or estimated. In this work we use observed values to seed the recurrent model.

3.2. Counterpropagation network (CPN)

The relatively simple, yet powerful counterpropagation algorithm sequentially combines the Kohonen self-organizing map and a Grossberg classification layer (Hecht-Nielsen, 1987). The combination leverages the unsupervised clustering self-organizing map with known output responses (a priori categories) to create a statistical mapping between predictor and response vectors (input-output pairs).

The CPN architecture consists of three nodal layers: input, Kohonen and Grossberg (Figure 4). All nodes in adjacent layers are connected via weights; matrix $\mathbf{w}_{ij}$ represents the weights between the I input and the J Kohonen nodes, likewise $\mathbf{u}_{jk}$ represents the weights linking the J Kohonen and K Grossberg nodes. The execution of the CPN is defined by two phases: a training phase and a prediction phase.

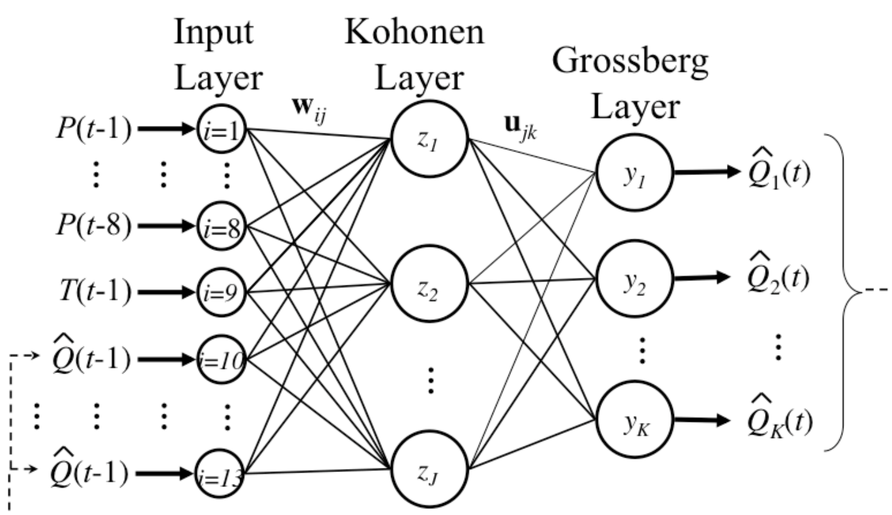

Figure 4. Architecture of counterpropagation network (CPN) with recurrent (feedback) connection (dashed line).

During training, the weights are iteratively adjusted to map the set of input predictor vectors, $\mathbf{x}$, to the set of associated response vectors, $\mathbf{Q}$, defined by some non-linear function $\mathbf{Q} = f(\mathbf{x})$, represented by the training data. A given input vector, $\mathbf{x}$, consisting of

M variables (x_1, x_2, …x_I), is passed to the hidden layer and a similarity metric is computed that compares the input vector and each weight vector, $\mathbf{w}_j$, associated with the Kohonen nodes. The Kohonen node with the weight vector most similar to the input vector is identified as the *winning* node and the weights associated with this winning hidden node are adjusted to be more similar to the input vector by:

$$\Delta\mathbf{w}_j = \begin{cases} \alpha(\mathbf{x} - \mathbf{w}_j), & \text{for } \; j = \text{winning node}, \\ 0, & \text{for } \; j \neq \text{winning node}, \end{cases}$$

where α is the Kohonen learning rate (α=0.7), $\mathbf{x}$ is the input vector, and $\mathbf{w}_j$ is the weight vector connecting the I input nodes to the j^{th} Kohonen node. Through a winner-take-all activation function, the winning Kohonen node propagates $z_{j=winner} = 1$ to the weights $\mathbf{u}_j$ of the Grossberg layer, while all other Kohonen nodes pass $z_{j\neq winner} = 0$. The network output $\hat{\mathbf{Q}}$ is computed as $\hat{Q}_k = \sum_{j=1}^{J} u_{jk} z_j$, where z_j is the activation value passed from the j^{th} Kohonen node, u_{jk} is the Grossberg weight connecting the j^{th} Kohonen node and the k^{th} Grossberg node and $\hat{Q}_k$ is the k^{th} component of the output vector, $\hat{\mathbf{Q}}$. The predicted flow vector $\hat{\mathbf{Q}}$ and observed flow vector $\mathbf{Q}$ are used to adjust the Grossberg weights as:

$$\Delta\mathbf{u}_j = \begin{cases} \beta(\mathbf{Q} - \hat{\mathbf{Q}}), & \text{for } \; j = \text{winning node}, \\ 0, & \text{for } j \neq \text{winning node}, \end{cases}$$

where β is the Grossberg learning rate (β=0.1). This process is repeated for all input-output pairs until the network has learned the input-output streamflow mapping defined by $\mathbf{Q} = f(\mathbf{x})$ to some user-defined convergence criterion (in this work, a summed root-mean-square error value less than 10^{-6}).

After convergence, the network weights are fixed and the CPN may be used for prediction. During this phase, input vectors that were not used to train the ANN are presented to the network for prediction. The number of hidden nodes used to generate predictions can be set to one for nearest neighbor or three for inverse distance weighted predictions (Besaw and Rizzo, 2007). Three winning nodes results in smoother predictions and was used for these applications.

Unlike the traditional feed-forward backpropagation ANNs, the counterpropagation algorithm cannot be over-trained and requires very little time for convergence. The algorithm was written in MatLab V. 7.4.0.287 (R2007a). For more details refer to (Besaw and Rizzo, 2007); pseudo-code is provided in Rizzo and Dougherty (1994).

Like the recurrent GRNN, the CPN architecture has been modified to incorporate a recurrent feedback loop (dashed lines in Figure 4). This allows antecedent predictions to be passed back to the network input layer to improve future predictions. As with the recurrent GRNN, this modification does not change the CPN algorithm; it simply adds information to the input layer when training and making predictions.

3.3. Autoregressive moving average with exogenous inputs (ARMAX)

ARMAX is a typical time series modeling approach frequently used in the flow forecasting literature for comparison with new flow prediction methods. A time-series analysis of the daily data, found the autoregressive and moving average components to be of order 2, while exogenous variables precipitation and temperature of orders 4 and 1, respectively (see Table 1). Thus our ARMAX model for the basins was expressed as:

$$\hat{Q}(t) = a_1 Q(t-1) + a_2 Q(t-2) + \sum_{i=1}^{4} b_{1i} P(t-i) + b_{21} T(t-1) + c_1 \varepsilon(t-1) + c_2 \varepsilon(t-2),$$

where $Q(t)$ is streamflow at time t, $P(t\text{-}i)$ is the precipitation associated with the previous i=1,2,…4 days, $T(t\text{-}1)$ is the one day prior average temperature, ε is the model error for the previous day (e.g. $\varepsilon(t\text{-}1)=\hat{Q}(t-1)-Q(t-1)$). The ARMAX model parameters have been found using a time-series analysis and the MatLab V. 7.4.0.287 (R2007a) System Identification Toolbox. The best fit autoregressive coefficients a_1 and a_2 are the associated with the antecedent streamflow; b_{1i} and b21 are the exogenous coefficients associated with precipitation *t-i* days prior and average temperature one day prior; c_1 and c_2 are the moving average coefficients.

3.4. Evaluation Criteria:

Several fundamental metrics are used to evaluate streamflow forecasting methods (Krause et al., 2005). The coefficient of determination, r^2, is the square of the sample correlation coefficient and is calculated as:

$$r^2 = \left(\frac{\sum_{i=1}^{N} \left(Q_i - \overline{Q}\right)\left(\hat{Q}_i - \overline{\hat{Q}}\right)}{\sqrt{\sum_{i=1}^{N} \left(Q_i - \overline{Q}\right)^2} \sqrt{\sum_{i=1}^{N} \left(\hat{Q}_i - \overline{\hat{Q}}\right)^2}} \right)^2$$

where $\hat{Q}_i$ and Q_i are the predicted and observed streamflow; $\overline{\hat{Q}}$ and $\overline{Q}$ are the mean predicted and observed streamflow respectively, and N is the total number of observations. The coefficient of determination describes how much of the observed variance is explained by the model. It ranges from 0 to 1; 0 implies no correlation, while a value of 1 suggests that the model can explain all of the observed variance.

Nash-Sutcliffe coefficient of Efficiency, *E,* measures the ability of a model to predict variables different from the mean and gives the proportion of the initial variance accounted for by the model (Nash and Sutcliffe, 1970). It is calculated as:

$$E = 1 - \frac{\sum_{i=1}^{N}\left(Q_i - \hat{Q}_i\right)^2}{\sum_{i=1}^{N}\left(Q_i - \overline{Q}\right)^2},$$

where E ranges from 1 (perfect fit) to $-\infty$. Values less than zero indicate that the observation mean would be a better predictor than the model.

Root mean square error (RMSE) is calculated as:

$$RMSE = \sqrt{\frac{\sum_{i=1}^{N}\left(Q_i - \hat{Q}_i\right)^2}{N}},$$

and is another common metric used for evaluating how closely predictions match observations. Values can range from 0 (perfect fit) to $+\infty$ (no fit) based on the relative range of the data.

In addition, measures of central tendency and dispersion based on prediction residuals and evaluation of conditional biasedness will be used to evaluate the methods. Mean residuals significantly different from zero often indicate a sub-optimal prediction method.

4. Results

4.1. Daily predictions using gauged streamflow observations

The goal of this work was predict streamflow in ungauged streams, using time-lagged streamflow predictions and local climate data as using inputs. In order to establish the prediction accuracies for these Vermont climate-flow systems, we first compare the four data-driven methods. The MLR, ARMAX, CPN and GRNN are used to forecast daily streamflow on two small basins; the Dog River, which has no impoundments, and Winooski River at Wrightsville, whose flow is regulated by a dam. In this proof of concept, precipitation lagged four days in time, temperature lagged one day and antecedent *observed* streamflows lagged by two days, were used as inputs to the models to forecast $Q(t)$. Seven years of data (total of 2,922 training patterns) were used to train and three years data (1,096 training patterns) were used to evaluate the methods (including both summer and winter months).

The GRNN smoothing parameter (σ^2) was determined through trial-and-error to be σ^2=7 (without normalization). This was the only parameter to optimize as the GRNN had as many nodes in the pattern layer, as there were training patterns. The MLR and ARMAX regression coefficients were determined using built-in MatLab functions (V. 7.4.0.287 R2007a). The CPN had no parameters to optimize, as an inverse distance-weighting algorithm with three winning nodes was implemented.

Summary statistics (prediction residuals and global error metrics (R^2, E, RMSE)) comparing the four model predictions against the observed streamflow at the Dog River and Winooski River are shown in Table 2. Additional scatter plots for the Dog River are shown in Figure 5. On the Dog River, CPN, GRNN and MLR model predictions have measures of central tendency (median) and dispersion that are statistically similar to the observed flow, as determined by the Wilcoxon-rank-sum and Brown-Forsyte tests respectively (type I error rate α=0.05); while the ARMAX prediction distributions are not. For the Winooski River, all models show statistically similar measures of central tendency and dispersion.

4.2. Recurrent CPN and GRNN

The CPN and GRNN implemented recurrent feedback connections (dashed lines in Figure 3 and Figure 4) to forecast Dog River streamflow at the hourly and daily time scale. The number of time-lagged inputs to the recurrent ANNs was determined through

Table 2. Comparing four streamflow prediction models in the Dog and Winooski Rivers.

	Dog River (m^3/s)					Winooski River at Wrightsville (m^3/s)				
	Q	**CPN**	**GRNN**	**MLR**	**ARMAX**	***Q***	**CPN**	**GRNN**	**MLR**	**ARMAX**
Mean	4.8	4.1	4.4	4.6	3.5	5.0	4.8	4.8	4.9	4.7
Median	3.1	2.6	2.7	3.3	2.2	2.8	2.7	2.7	2.9	2.6
Mode	1.0	1.3	1.3	1.7	0.4	0.8	1.0	1.4	1.1	0.7
St. Dev.	6.0	4.4	5.0	4.9	4.8	5.8	5.2	5.1	5.2	5.6
Min	0.4	0.4	1.0	-1.1	-2.1	0.23	0.3	0.6	0.0	0.0
Max	71	55	53	61	46	25.4	24.6	26.5	25.8	26.0
R^2	1	0.53	0.51	0.51	0.42	1	0.80	0.77	0.79	0.79
E	1	0.51	0.49	0.50	0.36	1	0.80	0.77	0.80	0.78
RMSE	0	4.2	4.3	4.3	4.8	0	2.6	2.8	2.6	2.7
R. Mean	0	-0.7	-0.4	-0.2	-1.3	0	-0.3	-0.2	-0.1	-0.3
R. Median	0	-0.1	0.1	0.4	-0.7	0	0.1	0.3	0.3	-0.1
R. St. Dev.	0	4.2	4.3	4.3	4.7	0	2.6	2.8	2.6	2.7

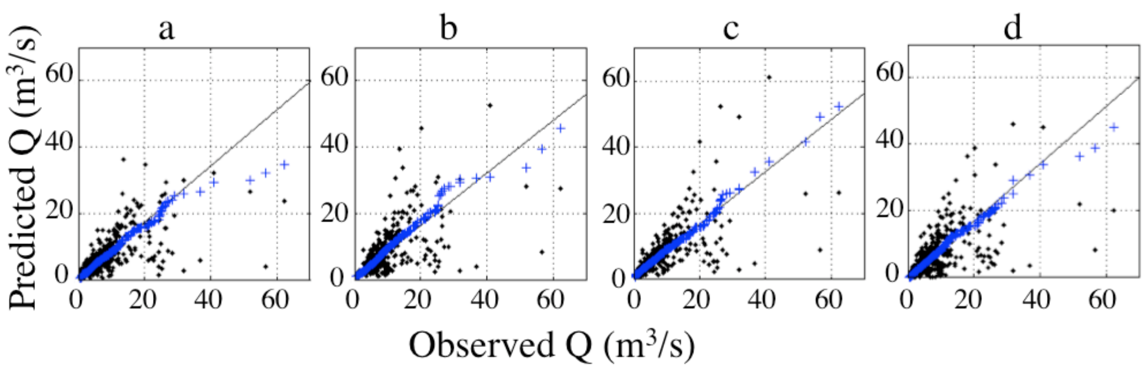

Figure 5. Comparison of predicted and observed streamflow using and (a) CPN, (b) GRNN, (c) MLR and (d) ARMAX predicted on the Dog River. Displayed are the flows (.), flow quantiles (+) and theoretical quantile line.

cross-correlation analysis. The hourly precipitation and flow were correlated up to 8 hours (Figure 2c), while streamflow was autocorrelated four hours. A daily temperature record was used as input because it was the finest temperature increment available. Thus, recurrent CPN and GRNN uses inputs of $P(t\text{-}1)$, $P(t\text{-}2)\ldots P(t\text{-}8)$, $T(t\text{-}1 \text{ day})$, $\hat{Q}(t\text{-}1)$, $\hat{Q}(t\text{-}2)\ldots\ \hat{Q}(t\text{-}4)$ to forecast hourly flow. In a similar manner, daily precipitation, temperature and flow recurrent CPN and GRNN inputs were found to be 4 days, 1 day and 2 days respectively. The ANNs were trained on eights years of input-output data pairs and made flow predictions for three years. All training and prediction data was from the Dog River. The hourly data consisted of 30,953 training and 9,612 prediction patterns, while daily data had 1,114 and 381 respectively. Both CPN and GRN used as many hidden/pattern nodes as there were training patterns. The GRNN smoothing parameter, σ^2, was found via trial and error to be 0.0089 and 0.00125 for the daily and hourly data, respectively.

Streamflow predictions were made for the summer months from 2004-2006. Figure 6 presents CPN and GRNN flow predictions over a 90-day window in the summer of 2004. This 90-day window was selected to show time-series predictions without compromising the readability of the figure. The qq-plots comparing $\hat{Q}$ and Q are provided for the 3 forecasting years. Evaluation criteria over three years of forecasting at the hourly and daily timescales are presented in Table 3.

4.3. Predicting ungauged streamflow

In this section the CPN and GRNN were trained on data from the Dog River to predict flow in the Winooski River at Montpelier) To more accurately predict flow at the Winooski River, climate data from the nearest weather station (Barre/Montpelier Airport) were used as inputs. Inputs include daily precipitation (lagged 4 days), temperature (lagged 1 day) and estimated flow (lagged 2 days). The GRNN smoothing parameter was determined previously (σ^2=0.0089). Thus, the recurrent ANNs were trained on the climate-flow records for one basin (Dog River) and used to predict flow at a nearby basin (Winooski River) using new climate data (Barre/Montpelier Airport) as the environmental driver.

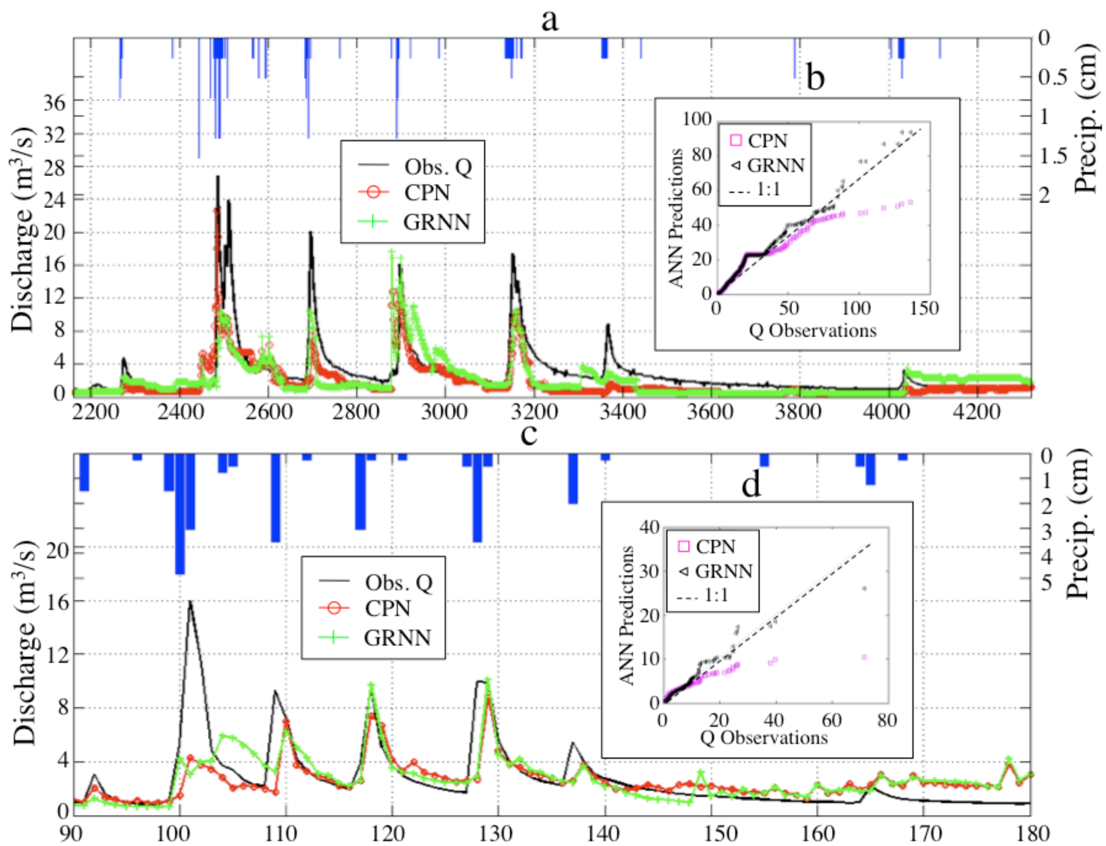

Figure 6. Time series streamflow observations (-) and ANN predictions at the (a) hourly and (c) daily timescales for a 90-day window of summer 2004. The inset figures represent the qq-plots for all predictions made for summers 2004-2006 at (b) hourly and (c) daily timescales.

Table 3. Hourly and daily error metrics for CPN and GRNN predictions at the Dog River.

	Hourly Data		Daily Data	
	CPN	GRNN	CPN	GRNN
R^2	0.5	0.45	0.29	0.29
E	0.28	0.28	0.16	0.02
RMSE	5.2	5.5	5.5	5.9
Corr	0.7	0.67	0.53	0.53
n	9,612	9,612	381	381

To account for the increase in drainage area from the Dog River (197 km^2) to the Winooski River (1028 km^2), the flow predictions were scaled by the ratio of areas (e.g. $Q_{winooski}$=Q_{dog}*($A_{winooski}$/A_{dog})). The relationship between bankfull discharge (Q_{bk}) and drainage area of basin (A) is well established in the literature as: Q_{bk}=eA^f (Leopold et al., 1964). Many empirical studies have found *f* to vary between 0.7 (semi-arid regions) and 1 (humid landscapes draining small catchments) (Vianello and D'Agostino, 2007).

Again, a 90-day snap shot of predicted and observed flow are presented in Figure 7. The qq-plot is also provided for the entire three years of forecasts. Error metrics comparing the two ANN algorithms for predicting daily flow in the Winooski River over the 3 forecasting years are presented in Table 4.

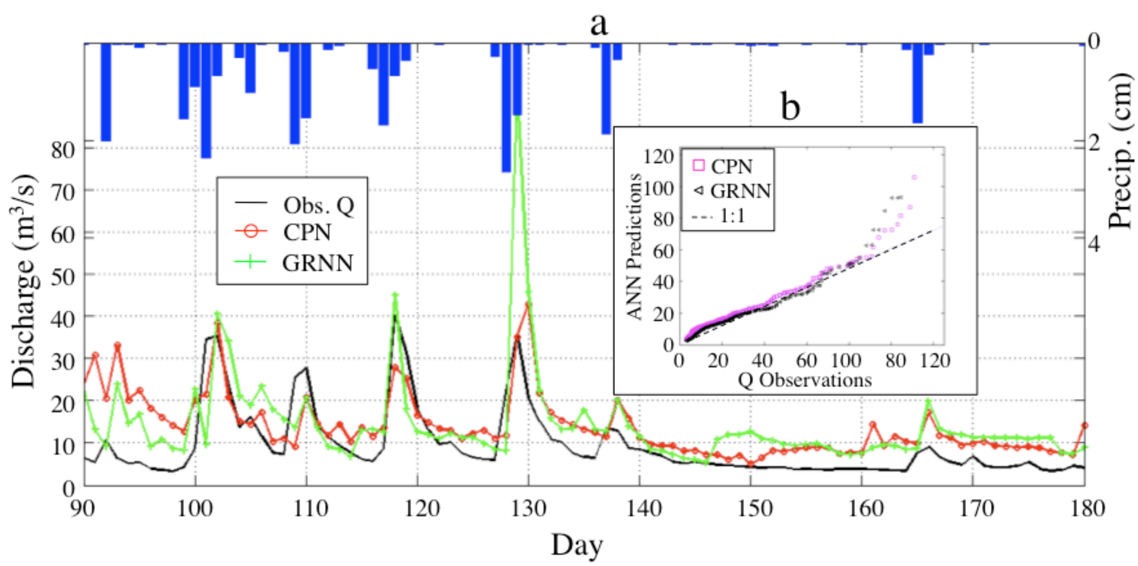

Figure 7. Time series streamflow observations (-) and ANN predictions on the Winooski River at Montpelier (a) over a 90 day forecast period (summer of 2004) and (b) qq-plots for the entire three years of prediction.

Table 4. Error metrics for the Winooski River at Montpelier flow predictions from 2004-2006.

	CPN	GRNN
R^2	0.24	0.16
E	0.12	-0.35
RMSE	18.0	22.7
Corr	0.49	0.37
n	540	540

5. Discussion

The goal of this work was to test the accuracy of two ANN methods for predicting streamflow in ungauged streams, using training data from a nearby, gauged stream. To predict on ungauged basins, model inputs consist of time-lagged streamflow predictions and local climate data. In order to establish the relative prediction accuracies for these climate-flow systems, we first compare daily streamflow forecasts of the CPN and GRNN algorithms with traditional methods.

5.1. Forecasts using observed antecedent observations

The forecasting models CPN, GRNN, MLR and ARMAX, using time-lagged antecedent streamflow *observation*s and climate data as inputs, have been used to predict daily streamflow on the Dog River and Winooski River at Wrightsville. In the Dog River, the CPN, GRNN and MLR prediction measures of central tendency (median) and dispersion (Table 2) are statistically similar to that of the observed streamflow, suggesting these estimation methods are superior to ARMAX in preserving the observed streamflow distribution. The estimated streamflow ranges (maximum – minimum) suggest that ARMAX over-smoothes the predictions. In addition, MLR and ARMAX predict negative streamflows, an undesirable effect resulting from linear combinations of training patterns. The CPN and GRNN residual central tendencies (median) are statistically more similar to zero than those of MLR and ARMAX, suggesting that these methods are less globally bias. Although the error metrics for CPN, GRNN and MLR are statistically similar (e.g. R^2=0.52, E=0.5 and RMSE=4.3), they are lower than those typically shown in the literature for these methods (e.g. R^2=0.80 E=0.80). This discrepancy is most likely due to the very rapid hydrological response of this basin and the aggradation of data to the daily time scale (Figure 2e). These findings suggest that the CPN, GRNN and MLR are equally well suited to predict streamflow in the unregulated (no reservoirs) streams such as the Dog River.

The error metrics at the Winooski River in Wrightsville, suggest all four methods produce statistically similar streamflow estimates and distributions when compared with the measured flow data. None of the prediction residuals have measures of central tendency statistically different than zero. The error metrics for these four methods are also statistically similar around R^2=0.79, E=0.78 and RMSE=2.7. These are similar to those typically provided in the literature suggesting all four methods accurately predict streamflow in the regulated Winooski River at Wrightsville basin.

Across both watersheds, the CPN, GRNN and MLR provide the most accurate and unbiased estimators of streamflow. There is no statistical difference in their predictions at these sites for these particular inputs (*P*, *T* and *Q*). It should be noted that the predictions for individual methods could have been improved had number of antecedent inputs been optimized for each method (as opposed to using time-series analysis principles). However, our goal was to allow for a fair evaluation by comparing the method accuracies using identical inputs.

Using antecedent streamflow observations as model inputs will always result in more accurate predictions than using antecedent streamflow predictions. However, using predicted flow rather than observed flow enables forecasts at any location within the river network (e.g. ungauged basins). Given the accuracies attained using *observed* antecedent streamflows as inputs, the relative accuracies associated with the recurrent ANNs can be evaluated.

5.2. Recurrent CPN and GRNN

The recurrent ANNs were used to prediction hourly and daily streamflow in the Dog River. Figure 6 shows a 90-day window of predictions and observations for the summer months of 2004. Both the recurrent CPN and GRNN capture the streamflow trends within this time frame. There are noticeably different accuracies between the two timescales. A comparison of prediction error metrics at the hourly and daily timescales (Table 3) reveals hourly models are superior. As expected, both the CPN and GRNN do a better job capturing the climate-flow relationship when trained on the hourly data (R^2 of 0.45 vs. 0.29). The improved flow predictions using hourly data is a function of the scale and basin characteristics. The Dog River basin tends to have very flashy responses to precipitation events. This flashiness is a function of numerous basin characteristics (e.g. drainage area, percent impervious surface, slope, soils, and geologic materials, etc.). Recall from Figure 2 and Table 1, the differences in characteristic lags times between P and Q. The hourly data reveal that P and Q are correlated up to 8 hours. This was also a typical length of time between the peak rainfall and peak storm flow, as revealed by hydrographs (not shown). Thus, the daily data is not capturing the temporal relationship between P and Q (see Figure 2b and e). This loss of temporal information is the root cause of the difference in predictive capabilities at the hourly and daily timescales. The reduced prediction capability at the daily scale is not a result of the forecasting algorithms, but is rather a function of the data measurement scale in this particular basin.

Both the GRNN, and to a greater extent, the CPN predictions contain conditional bias in that they tend to under predict high flows (Figure 6b and d). This is to be expected as the majority of recorded data (both training and prediction) consist of base flow events. In addition to training on all summer data, hourly ANNs were also trained only on storm events from 1996-2003 (results not shown). This reduced the number of training patterns from 30,953 to 6,723. Although the summary statistics were not significantly improved (R2=0.52, E=0.32 and RMSE=5.2, but again keep in mind the majority of flows are base flows), the observed and predicted distributions were not statistically different (as determined with a two sample Kolmogovnov-Smirnov test). This suggests training on storm events improves the ANNs' abilities to forecast peak flows.

Predicting streamflow using recurrent ANNs that feedback lagged *predictions* of flow, rather than observations, does reduce prediction accuracies. As a demonstration, daily CPN predictions on the Dog River using lagged observations of Q as inputs, had R^2=0.53, E=0.51 and RMSE=4.2, while the daily recurrent CPN, using lagged $\hat{Q}$ as inputs, had R^2=0.29, E=0.16 and RMSE=5.2. These statistically different metrics were expected because the recurrent algorithms may be compounding errors when using antecedent predictions to drive future predictions. However, these feedbacks are essential in order to make reasonable forecasts in ungauged basins.

At the onset of this study, the climate and flow records were separated into summer and winter seasons due to Vermont's season hydrological responses. Although all predictions made using the recurrent ANNs were only made on the summer months, the time series analysis and ANN methods would prove equally applicable to forecast winter flows; given the analyses are rerun to determine the correct lag periods for inputs of P, T and $\hat{Q}$.

The data-driven methods presented here for predicting streamflow must be trained on some known (observed) set of climate-flow data. Therefore, to advance a methodology for predicting flow in an ungauged basin, the recurrent ANNs were also used to predict daily flow in an entirely different watershed.

5.3. ANN transferability and scaling

In the preceding section, the Dog River and associated climate-flow record was used to train a CPN and GRNN. In this application, we use these ANNs to predict flow with input climate data from the nearby Winooski River at Montpelier. To account for the increase in drainage area from the Dog River to Winooski River, a simple scaling algorithm was utilized. In this particular case, predictions were scaled up to a larger basin; but the predictions may just as easily be scaled down to a smaller basin. The error metrics (Table 4) indicate the CPN outperforms the GRNN for this application. Once again, the aggregation of data to the daily scale plays an important role in these prediction accuracies. Predictions would be improved had the climate-flow relationships been better captured in the data. The qq-plots (Figure 7) show that both the CPN and GRNN do an excellent job of producing flows prediction distributions similar to the observed flow distribution. This is encouraging given that the ANNs were trained on data from an different watershed. Predictions of the extremely high flows deviate from the theoretical quantile line. This conditional biasedness could once again be solved by training the ANNs only on storm events (as previously discussed).

The transfer of the CPN methodology from one basin to another, and subsequent flow scaling by area, does not result in a significant reduction in prediction accuracies. Training the CPN on daily data from the Dog River and predicting in the same basin resulted in a CPN R^2 of 0.29. Using the Dog River training data and predicting flow on the Winooski River at Montpelier resulted in a CPN R^2 of 0.24. This is primarily a function of 1) the use of measured local climate data as the driver (inputs) and 2) the fact that the network was trained on a sufficiently large number of regional climate-flow data (e.g. flood and low flow events) over a time period where landuse did not change significantly.

The CPN and GRNN were selected due to their guaranteed convergence and avoidance of stochastic training. The determination of σ^2 for GRNN algorithm is the only source of training iteration. Numerous trial-and-error runs are required to determine the GRNN's optimal σ^2. As the CPN does not require this iterating, its training speed proves to be superior to that of the GRNN. However, this speed comes as a tradeoff as the GRNN (with optimized σ^2) can be a more flexible forecasting method, by combining outputs from more training patterns to compute a prediction.

6. Conclusions

Eleven years of NCDC climate and USGS flow records from several stations within Vermont's Winooski River Basin have been used to make advances in streamflow forecasting. A simple methodology, using time-series analysis, has been used to determine the appropriate lag periods between input and output variables.

Motivated to predict streamflow in ungauged basins, recurrent ANN algorithms were developed and implemented to forecast streamflow using lagged flow predictions, rather than lagged observations, as inputs. As expected, using antecedent flow predictions to predict future flows is less accurate than using antecedent observations. However, since observed streamflow is not available at the majority of small (ungauged) basins, using antecedent predictions to make future predictions produces is more accurate and reliable, than using climate data alone. In addition, we have provided a straightforward to scaling technique to predict flow in basins of various drainage area.

The combination of recurrent ANNs with scaling demonstrates these methods may be applied to predict streamflow in ungauged basins. As a proof-of-concept, we trained the ANNs on climate-flow data from the Dog River and predicted flow in the nearby Winooski River (using local climate data as inputs). Predictions were scaled account for the difference in basin areas and predictive accuracies are within the range of those found for ANNs trained and predicted using climate and flow data within the same basin.

By selecting ANNs that always converge and avoid stochastic training algorithms, these methodologies are straightforward to execute and widely applicable to small ungauged basins. As such, they would prove useful to watershed and water resources management stakeholders.

7. Acknowledgements

Thank you GEOL 371 class for reading this manuscript. Your comments are most appreciated!

8. References

Adamowski, J.F., 2008. Development of a short-term river flood forecasting method for snowmelt driven floods based on wavelet and cross-wavelet analysis. Journal of Hydrology, 353: 247-266.

Albers, J., 2000. Hands on the Land, A History of the Vermont Landscape. MIT Press, Cambridge, MA.

Aytek, A., Asce, M. and Alp, M., 2008. An application of artificial intelligence for rainfall-runoff modeling. Journal of Earth Syst. Sci., 117(2): 145-155.

Besaw, L.E. and Rizzo, D.M., 2007. Stochastic Simulation and Spatial Estimation with Multiple Data Types using Artificial Neural Networks Water Resources Research, 43, W11409, doi:10.1029/2006WR005509.

Box, G. and Jenkins, G., 1970. Time series analysis: Forecasting and control. Holden-Day, San Francisco, CA.

Chaloulakou, A., Assimacopoulos, D. and Lekkas, T., 1999. Forecasting daily maximum ozone concentration in the Athens basin. Environmental Monitoring and Assessment, 56(97-112).

Chang, F.-J., Chang, L.C. and Huang, H.-L., 2002. Real-time recurrent learning neural network for stream-flow forecasting. Hydrological Processes, 16: 2577-2588.

Chang, F.J. and Chen, Y.-C., 2001. A counterpropagation fuzzy-neural network modeling approach to real time stream flow prediction. Journal of Hydrology, 245: 153-164.

Chang, F.J., Hu, H.F. and Chen, Y.C., 2001. Counterpropagation fuzzy-neural network for streamflow reconstruction. Hydrological Processes, 15(2): 219-232.

Cigizoglu, H.K., 2003. Estimation, forecasting and extrapolation of river flows by artificial neural networks. Hydrological Sciences, 48(3): 349-361.

Cigizoglu, H.K., 2005a. Application of generalized regression neural networks to intermittent flow forecasting and estimation. Journal of Hydrologic Engineering, 10(4): 336-341.

Cigizoglu, H.K., 2005b. Generalized regression neural network in monthly flow forecasting. Civil Engineering and Environmental Systems, 22(2): 71-84.

Connor, J.T., Martin, R.D. and Atlas, R.D., 1994. Recurrent neural networks and robust time series prediction. IEEE Transactions on Neural Networks, 5(2): 240-254.

Doolan, B., 1996. The Geology of Vermont. Rocks and Minerals, 71: 218-225.

Firat, M., 2008. Comparison of artificial intelligence techniques for river flow forecasting. Hydrol. Earth Syst. Sci, 12: 123-139.

Firat, M. and Gungor, M., 2008. Hydrological time-series modelling using an adaptive neuro-fuzzy inference system. Hydrological Processes, 22: 2122-2132.

Govindaraju, R.S., 2000a. Artificial Neural Networks in Hydrology I: Preliminary Concepts. Journal of Hydrologic Engineering, 5(2): 115-123.

Govindaraju, R.S., 2000b. Artificial Neural Networks in Hydrology II: Hydrogeologic Applications. Journal of Hydrologic Engineering, 5(2): 124-137.

Govindaraju, R.S. and Ramachandra, R.A., 2000. Artificial Neural Networks in Hydrology. Kluwer Academic Publishers, Dordrecht, The Netherlands.

Hackett, W.R. and Bierman, P.R., 2009a. Quantifying seventy years of landuse change in the Winooski River Basin, northern Vermont. Journal of Environmental Management, In preparation.

Hackett, W.R. and Bierman, P.R., 2009b. Winooski River trends of seventy years of flow records.

Hecht-Nielsen, R., 1987. Counterpropagation Networks. Applied Optics, 26(23): 4979-4984.

Hijmans, R.J., Cameron, S.E., Parra, J.L., Jones, P.G. and Jarvis, A., 2005. Very high resolution interpolated climate surface for global land areas. International Journal of Climatology, 25: 1965-1978.

Hsieh, W.W., Yuval, L.J.Y., Shabbar, A. and Smith, S., 2003. Seasonal prediction with error estimation of Columbia river streamflow in British Columbia. Journal of Water Resources Planning and Management - ASCE, 129(2): 146-149.

Hsu, K., Gupta, H.V. and Sorooshian, S., 1995. Artificial neural network modeling of the rainfall-runoff process. Water Resources Research, 31(10): 2517-2530.

Hsu, K.L., Gupta, H.V., Sorooshian, G.S. and Imam, B., 2002. Self-organizing linear output map (SOLO): An artificial neural network suitable for hydrologic modeling and analysis. Water Resources Research, 38(12): 1312, doi:10.1029/2001WR001118.

Hu, T.S., Lam, K.C. and Thomas, N.G., 2005. A modified neural network or improving river flow prediction. Hydrological Sciences, 50(2): 299-318.

Imrie, C.E., Durucan, S. and Korre, A., 2000. River flow prediction using artificial neural networks: generalisation beyond the calibration range. Journal of Hydrology, 233: 138-153.

Jeong, D.I. and Kim, Y.-O., 2005. Rainfall-runoff models using artificial neural networks for ensemble streamflow prediction. Hydrological Processes, 19: 3819-3835.

Khalil, A.F., McKee, M., Kemblowski, M. and Asefa, T., 2005. Basin scale water management and forecasting using artificial neural networks. Journal of American Water Resources Association, 41(1): 195-208.

Kingston, G.B., Maier, H.R. and Lambert, M.F., 2005. Calibration and validation of neural networks to ensure physically plausible hydrological modeling. Journal of Hydrology, 314: 158-176.

Kisi, O., 2005. Daily river flow forecasting using artificial neural networks and auto-regressive models Turkish Journal of Engineering and Environmental Sciences, 29(1): 9-20.

Kisi, O., 2008. River flow forecasting and estimation using different artificial neural network techniques. Hydrology Research, 39(1): 27-40.

Krause, P., Boyle, D.P. and Base, F., 2005. Comparison of different efficiency criteria for hydrological model assessment. Advances in Geosciences, 5: 89-97.

Leopold, L.B., Wolman, M.G. and Miller, J.P., 1964. Fluvial Processes in Geomorphology. Freeman, San Francisco, 522 pp.

Maier, H.R. and Dandy, G.C., 2000. Neural networks for the prediction and forecasting of water resources variables: a review of modelling issues and applications. Environmental Modelling & Software, 15: 101-124.

Makkeasorn, A., Chang, N.B. and Zhou, X., 2008. Short-term streamflow forecasting with global climate change implications - A comparative study between genetic programming and neural network models. Journal of Hydrology, 352: 336-354.

McKerchar, A.I. and Delleur, J.W., 1974. Applications of seasonal parametric linear stochastic models to monthly flow data. Water Resources Research, 10: 246-255.

Moradkhani, H., Hsu, K.-L., Gupta, H.V. and Sorooshian, S., 2004. Improved streamflow forecasting using self-organizing radial basis function artificial neural networks. Journal of Hydrology, 295: 246-262.

Nash, J.E. and Sutcliffe, J.V., 1970. River flow forecasting through conceptual models, Part I - A discussion of principles. Journal of Hydrology, 10: 282-290.

Phien, H.N., Huong, B.K. and Loi, P.D., 1990. Daily forecasting with regression analysis. Water SA, 16(3): 179-184.

Rajurkar, M.P., Kothyari, U.C. and Chaube, U.C., 2002. Artificial neural networks for daily rainfall-runoff modelling. Hydrological Sciences, 47(6): 865-877.

Rizzo, D.M. and Dougherty, D.E., 1994. Characterization of aquifer properties using artificial neural networks: Neural kriging. Water Resources Research, 30(2): 483-497.

Schilling, K.E. and Wolter, C.F., 2005. Estimation of streamflow, baseflow and nitrate-nitrogen loads in Iowa using multiple regression models. Journal of American Water Resources Association, 41(6): 1333-1346.

Singh, P. and Deo, M.C., 2007. Suitability of different neural networks in daily flow forecasting. Applied Soft Computing, 7: 968-978.

Specht, D.F., 1991. A general regression neural network. IEEE Transactions on Neural Networks, 2(6).

Tangborn, W.V. and Rasmussen, L.A., 1976. Hydrology of the North Cascades region, Washington - Part 2: a proposed hydrometeorological streamflow prediction method. Water Resources Research, 12: 203-216.

Tolland, L., Cathcart, J.G. and Russel, S.O.D., 1998. Estimating the Q100 in British Columbia: a practical problem in forest hydrology. Journal of Water Resources Association, 34: 787-794.

Vianello, A. and D'Agostino, V., 2007. Bankfull width and morphological units in an alpine stream of dolomites (Northern Italy). Geomorphology, 83: 266-681.

Wang, W., Van-Gelder, P.H.A.J.M., Vrijling, J.K. and Ma, J., 2006. Forecasting daily streamflow using hybrid ANN models. Journal of Hydrology, 324: 383-399.

Yurekli, K., Kurung, A. and Ozturk, F., 2005. Testing residuals of an ARIMA model on the Cekerek stream watershed in Turkey. Turkish Journal of Engineering and Environmental Sciences, 29: 61-74.

Zadeh, L.A., 1965. Fuzzy sets. Information and Control, 8(3): 338-353.

Zealand, C.M., Burn, D.H. and Simonovic, S.P., 1999. Short term streamflow forecasting using artificial neural networks. Journal of Hydrology, 214: 32-48.